1

A Telemanipulation System for Psychophysical Investigation of Haptic Interaction

B. J. Unger,* R. L. Klatzky,‡ and R. L. Hollis*

Carnegie Mellon University
Pittsburgh, Pennsylvania, USA

Abstract

We report an experimental high-fidelity system for making psychophysical measurements on human operators performing real, virtual, and real-remote 3-D haptic manipulation tasks. Operators interact with task environments through six-degree-of-freedom (6-DOF) Lorentz magnetic levitation haptic devices. This arrangement allows the operator to exert and experience real, virtual, and real-remote forces/torques using the same 6-DOF master device. In the virtual task scenario, interactions are rendered haptically. In the real task scenario, the manipulandum of the haptic device interacts by direct mechanics with a real environment. In the remote-real scenario, interactions with a remote real task environment are mediated through a 6-DOF Lorentz magnetic levitation slave device carried by a 6-DOF robot arm. In all three scenarios, visual feedback is provided by a graphical display. The system records accurate positions/orientations and forces/torques as a function of time. These records can be parsed automatically and analyzed off-line to evaluate operator performance.

1 Introduction

The study of haptic feedback for task performance in real and virtual environments has received considerable attention in recent years. Many haptic displays have been tested using various performance criteria.

The fidelity of a particular haptic display is often measured in terms of kinematic and dynamic design constraints such as force bandwidth and dynamic range [1] or frequency response and steady state accuracy. Other tests have concentrated on the operator's ability to perform specified tasks. Analysis of task performance has generally focused on binary failure/completion criteria, accuracy [2] or completion time analysis [3]. Whereas simple measurements of task performance demonstrate gains when hap-

tic feedback is employed, they fail to delineate the underlying strategies used by the subject in attaining the goal. More sophisticated analysis employing force/torque and position/orientation data collected throughout a task provides richer, quantifiable performance metrics.

By examining these data recorded continuously during the procedure, a larger task can be broken into subtasks, allowing quantitative analysis of the effect of different parameters on each subtask. Identification of important subgoals, user force and position strategies, and the influence of device parameters may then provide guidance for improved interface design and further understanding of the psychophysics of haptics. For example, operator performance during peg-in-hole placement tasks can be studied [4, 5, 6]. Such studies provide a point of reference for the goal of understanding human manipulation strategies.

Performance of tasks involving contact in three dimensions involves discrimination of point, edge and face hard contacts during motion in 6 DOFs. To compare task performance in virtual, real, and real-remote (telemanipulation) scenarios, it is important that haptic feedback realistically represents this environment. Device limitations, such as stiffness range, position resolution and bandwidth, may result in noticeable deviations from the ideal haptic experience. The system described in this paper aims to minimize these effects by using both a master and slave which are high in haptic fidelity.

2 Lorentz Magnetic Levitation

Our approach to telemanipulation uses Lorentz levitation [7] for both the master and slave devices. A system of this type was first demonstrated at the University of British Columbia [8]. The devices incorporate levitated rigid bodies or "flotors" which are free to move in 6 DOFs over some limited range of motion. Depending on design, flotors can have low masses which give high motion bandwidths; can have low inductances, which yield high force bandwidths,

---

*The Robotics Institute, School of Computer Science.
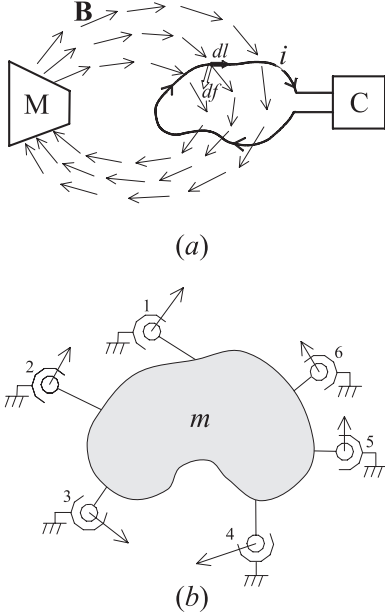‡ Department of Psychology, Human Computer Interaction Institute.

(a)

(b)

Figure 1: (a) Generalized Lorentz actuator, (b) Lorentz levitation of a body of mass m. The position/orientation of the body is measured by sensors (not shown).

and are free of static friction.

The magnetic Lorentz force F_L per unit length of conductor is given by $F_L = |\mathbf{i} \times \mathbf{B}|$, where $\mathbf{i}$ is the current vector in the conductor and $\mathbf{B}$ is the flux density vector. In contrast with the Maxwell force employed in magnetic bearings, the Lorentz force allows bi-directional forces with simple linear control.

The term "Lorentz levitation" refers to the levitation of a body by means of Lorentz forces generated in current-carrying conductors immersed in magnetic fields. For stable levitation in 6 DOFs, a minimum of six actuators and the ability to sense motion in 6 DOFs is required [7]. The technology for Lorentz levitation was developed at the IBM T. J. Watson Research Center in the mid-1980s [9].

Many different actuator designs are possible, with windings and magnets arranged in three-dimensional configurations. Figure 1(a) illustrates a generalized Lorentz actuator where a current i flowing in a circuit through a controlled source C interacts with a fixed field $\mathbf{B}$ produced by a magnetic circuit M. Particular designs may have localized windings and magnets, although these elements may be distributed and more than one winding can share the field from a given magnet structure. Examples of Lorentz actuators include loudspeaker voice coils and rotary disk drive actuators. Referring to Fig. 1(b), a body is levitated by at least six Lorentz actuators. Each actuator produces a distinct force vector while allowing full 6-DOF motion over a limited range. For each actuator
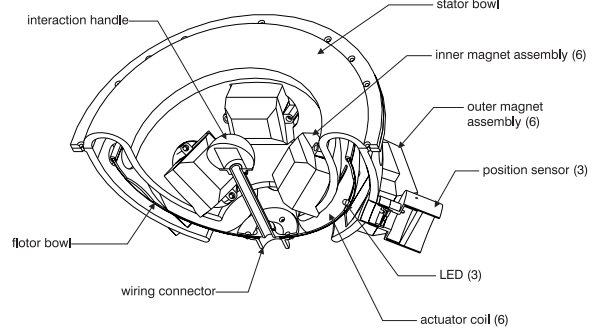

Figure 2: Lorentz magnetic levitation haptic master cut-away view of design.

k, the current i_k interacts with the local field $\mathbf{B}_k$ to produce a force $\mathbf{f}_k = -i_k \oint \mathbf{B}_k \times \mathbf{dl}$, where $\mathbf{dl}$ is an element of wire in the coil and the line integral is taken over the entire coil.

The actuator set $\{\mathbf{f}_k, k = 1, ..., 6\}$ must be arranged so that no two actuators share a common line of action. The wrench vector $w = [f_x, f_y, f_z, \tau_x, \tau_y, \tau_z]^T$ acting on the flotor is given by $w = AI$ where $I = [i_1, i_2, ..., i_6]^T$ is the vector of coil currents and A is a (non-singular) 6×6 geometric transformation matrix.

The position and orientation of the levitated body with respect to ground can be measured by capacitance, inductance, or by optics. For small rotations, the position-orientation vector $p = [x, y, z, \theta_x, \theta_y, \theta_z]$ is given by $p = Sq$ where $q = [q_1, q_2, ..., q_6]^T$ is the vector of sensor measurements and S is another 6×6 geometric transformation matrix.

Control is best accomplished globally with respect to an orthogonal $[x, y, z]$ frame $\mathcal{F}$ embedded in the flotor. A linearized dynamic model and control strategies for Lorentz levitators can be found in [10]. More recently, a new control approach has been proposed by Fasse [11].

2.1 Telemanipulation master device

To effectively compare task performance in real and virtual scenarios, it is necessary to use a rendering device capable of providing realistic haptic sensation. Ideally, such a device should have high position and force bandwidths, fine position resolution and high range of impedance. Six DOFs are necessary to emulate the forces and torques encountered in real 3D tasks. The magnetic levitation haptic master device used in this system, shown in Fig. 2, provides such a platform [12]. The device has a hemispheric actuator assembly, optical position sensors, electronics, and realtime computer.

The flotor has six coils embedded in a hemispheric aluminum shell enclosed within the stator's fixed magnet assemblies. Current in each coil interacts
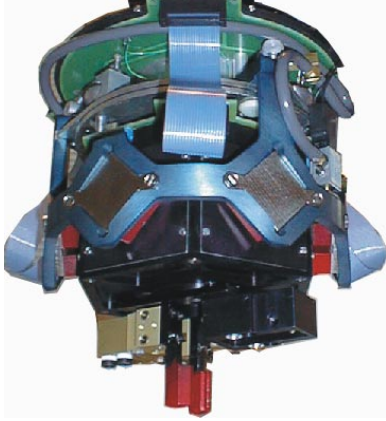
Figure 3: Magic Wrist slave device.

Figure 4: Coarse-fine slave.

with the strong magnetic fields of the enclosing magnets to produce six independent Lorentz forces, providing an arbitrary force/torque wrench on the flotor, and hence to the attached manipulandum and the operator's hand. Three LEDs on the flotor imaged by lenses and sensed by fixed optical sensors provide position and orientation information with resolutions of 5-10 μm, depending on position in the workspace. Because of the low flotor mass and freedom from static friction, a position bandwidth of ($\sim$125 Hz at ±3 dB) is achieved [12]. Maximum stiffness is approximately 25 N/mm in translation and 50.0 Nm/rad in rotation [12]. 6-DOF motion of the handle has a range approximately that of comfortable fingertip motion with the wrist stationary (±12 mm translation and $\pm7°$ rotation in all directions).

2.2 Telemanipulation slave device

The telemanipulation slave device in our system is shown in Fig. 3. The IBM Magic Wrist, developed in the late 1980's, is a 6-DOF fine motion device that can be attached to the last link of a conventional robot to give the robot extraordinary compliant motion and positioning capabilities. In our system, the wrist is attached to the tooling mount of a PUMA 560 industrial robot (Fig. 4).

In this device, the flotor is levitated by six Lorentz actuators arranged at 60° intervals around a horizontal ring. Each actuator has a line of action at 45° with respect to the vertical axis of symmetry. The permanent magnet structures of the actuators are attached to inner and outer stators which in turn are attached to the distal link of the robot arm coarse manipulator, whereas the coils of each actuator are contained in the thin, hexagonal flotor shell. The position and orientation of the flotor with respect to the stator is sensed by a triplet of optical beams directly projecting from the stator to a corresponding set of two-axis position-sensing photodiodes (PSDs) attached to the

inside of the flotor. A set of three thin flexible ribbon cables provide power and signals to and from the flotor. The flotor has a motion range of ±5 mm in translation and $\pm4°$ in rotation, a position resolution of approximately 1 μm, and a bandwidth of around 50 Hz.

3 Telemanipulation System

Our coarse-fine telemanipulation system allows an operator to grip a master manipulandum (Fig. 2) and apply and feel the force/torque wrench generated by a tool held at the tip of the slave wrist (Fig. 3) carried by a robot (Fig. 4).

Figure 5 is a block diagram showing connections between the system components. The magnetic levitation master is controlled by an AMD XP 2000+ (1.67 GHz) computer. The master's position sensors are read by an Acromag IP330 A/D card (16 bits, 8 μs conversion time), and its amplifiers are driven by an Acromag IP220 D/A card (12 bits, 8 μs settling time). Controllers typically run at 1-4 KHz, depending on complexity.

The coarse positioning robot is a 6-DOF PUMA 560, controlled by a Motorola VME 162-23 computer running RCCL/RCI software. The controller communicates with the PUMA via its Unimate controller. The RCCL/RCI software allows the PUMA's tool mount to be servoed to a specified position in its world coordinate frame. The Magic Wrist is attached to the PUMA tool mount giving the slave manipulator a total of 12 DOF's. The wrist is controlled by a 1-4 KHz servo loop running on another AMD XP 2000+ (1.67 GHz) computer with IP330 A/D converter and IP220 D/A converter. A small, pneumatically-activated gripper mounted on the wrist provides an end effector.
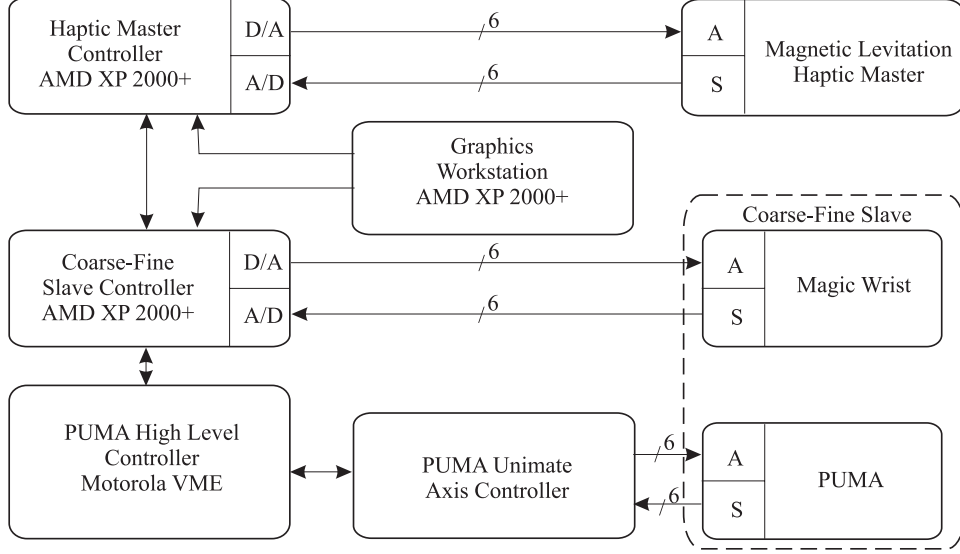
Figure 5: Coarse-fine telemanipulation system components.

Control of both the wrist and PUMA is governed by a higher level manager, running on the same AMD XP 2000+ computer that runs the wrist servo loop. The manager communicates with the VME computer at approximately 60 Hz to adjust the position/orientation of the PUMA. Communication between the haptic master controller and the coarse-fine manager currently runs at ∼1000 Hz over an Ethernet link. We are moving to a Firewire (IEEE 1394) link, which will afford much faster communication rates.

A PC-based graphics workstation (third AMD XP 2000+ computer with a GeForce4 TI 4600) is connected to both the master and coarse-fine slave via Ethernet and Firewire. The workstation provides a point of central operation and has several graphical user interface tools for controlling its various components. It also provides a visual rendering of the slave end effector's operational environment or a virtual environment. In addition, the graphics workstation is responsible for rendering haptic feedback using physical modelling software, independent of the slave system. Positions/orientations from the workstation simulation (x_{sim}) and haptic master controller (x_{dev}) are exchanged as vectors and act as impedance control set points. Position error ($x_{sim} - x_{dev}$) and velocity feedback (v_{dev} or v_{sim}) provide a virtual spring-damper connection between the systems. The forces acting on the haptic master (f_{dev}) and present in the virtual representation f_{sim} are given by

$$f_{dev} = K_p \left(x_{sim} - x_{dev} \right) + K_v v_{dev,}$$

and

$$f_{sim} = K_{spring} \left(x_{dev} - x_{sim} \right) + K_{damp} v_{sim} + f_{other,}$$

where f_{other} are contact forces in the simulation. K_{spring} and K_{damp} are gains of the virtual spring-damper in the simulation and K_p and K_v are gains for the virtual spring-damper of the haptic master.

Symmetric bi-lateral control is implemented. That is, force/torque feedback between the haptic master and the end effector on the slave wrist is implemented by passing position/orientation information between their respective servo loops and having each magnetic levitation device servo to the other's position.

To position the slave it is necessary to map the coordinate system of the master's manipulandum to the slave's world coordinates. The haptic master world frame of reference, $\mathcal{W}$, is considered to be coincident with its stator frame. A frame attached to the master's manipulandum, $\mathcal{F}$, is coincident with $\mathcal{W}$ at rest (floating in the center of its workspace). The slave frame of reference $\mathcal{L}$ is also considered to be coincident with its own stator frame $\mathcal{M}$ at rest. $\mathcal{W}$ and $\mathcal{M}$ can be considered coincident for the purposes of teleoperation. The transformation $\mathbf{T}_F^W$ that describes the position of the master's manipulandum $\mathbf{v}$ in the master's world space coordinates is thus $\mathbf{v}^W = \mathbf{T}_F^W \mathbf{v}^F$. The transformation is scaled by some factor $\mathbf{c}$ and the desired position of the slave end effector $\mathbf{v}^M$ in its world space coordinates is determined by $\mathbf{v}^M = \mathbf{c}\mathbf{T}_F^W \mathbf{v}^F$. The tool mount position/orientation of the PUMA arm is determined relative to the position of the wrist frame of reference. At start up, the PUMA's tool mount frame $\mathcal{N}$ is considered its global world frame $\mathcal{P}$. This is displaced from the wrist global frame of reference by a translation $\mathbf{T}_M^P$ which transforms a vector in the fixed
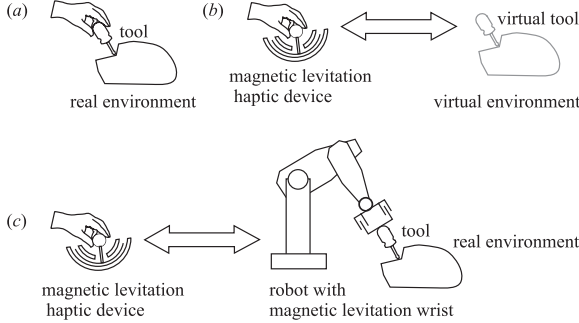
4

Figure 6: Three haptic interaction scenarios: (a) interaction with a real environment using a real tool, (b) interaction with a virtual environment using a virtual tool, and (c) interaction with a remote real environment using a real tool.

wrist frame $\mathcal{M}$ to the PUMA's global world frame $\mathcal{P}$: $\mathbf{v}_P = \mathbf{T}_M^P \mathbf{v}_M$. Since the PUMA's tool mount frame is expected to track the position of the center of the wrist flotor, $\mathbf{T}_L^N = \mathbf{T}_M^P$. Therefore a vector in PUMA world space $\mathbf{v}^{\mathbf{P}}$ is determined from the master by $\mathbf{v}^{\mathbf{P}} = \mathbf{T}_M^P \mathbf{c} \mathbf{T}_F^W \mathbf{v}^F$.

Various means are used to coordinate coarse and fine motion. In tracking mode, the PUMA arm simply tracks the position of the center of the wrist workspace, providing a large virtual workspace for the wrist's flotor. One can, for example, grasp the wrist flotor and use it to guide the PUMA through large motions. When the PUMA is moved from the haptic master, scaling, indexing, and rate control is used to compensate for the master's limited motion range [8].

4   A Platform for Psychophysical Evaluation

To date we have performed a series of haptic psychophysical measurements and analysis in two separate haptic scenarios: (a) real forces with visual display, and (b) virtual forces with visual display. In both of these scenarios, operators were asked to perform a 3D peg-in-hole assembly. We are using the Lorentz levitation telemanipulation system described in this paper to perform additional psychophysical tests in (c) the remote-real scenario (see Fig. 6).

An important aspect of our method is that the real-force, virtual-force, and remote-real scenarios are matched with respect to the visual display and the visible and felt manipulandum.

Real force scenario: This scenario was devised by attaching a real square peg to the bottom of the flotor of the haptic master. A block with a square hole

was mounted on a JR3 force/torque sensor* situated below the flotor [6].

The operator's task in this scenario was to place the real peg in the real hole with the haptic master's actuators inactive, directly experiencing the contact forces and torques generated by the interaction of the real peg with the real hole. The sensors in the master remained operative, and position/orientation data were used to update the visual display. Forces, torques, positions, and orientations were measured and logged at 100 Hz.

Virtual force scenario: The system models interactions with a 3D physically simulated rigid-body world in which objects dynamically react to collisions, friction, gravity, or other forces. The graphics workstation runs the Coriolis™ dynamic simulation package which calculates forces and motions of non-interpenetrating rigid bodies in space due to Newtonian mechanics, contact constraints, collisions, and friction in near real time [13].

In formal experiments with student volunteers, the haptic master was used to display the environment for a 3D peg-in-hole manipulation. Again, data were recorded at 100 Hz.

Remote-real scenario: This scenario utilizes the full telemanipulation system described in this paper, enabling quantitative comparisons between real, virtual, and real-remote haptic interaction. Direct interaction [Fig. 6 (a)], is the ideal with which computer-mediated interactions (b) and (c) are to be compared. If we characterize the computer-mediated interactions in terms of a multi-dimensional filter function $\mathcal{F}: 0 \leq \mathcal{F} \leq 1$, where $\mathcal{F} = 1$ represents haptic transparency, then in (b), the haptic experience is filtered (reduced) by the electromechanics of the haptic device $\mathcal{F}_h$, and by the accuracy of the simulated environment $\mathcal{F}_e$. In (c), the identical haptic device is used, but the filtering property $\mathcal{F}_e$ of the virtual environment is swapped for that of a second device, a magnetic levitation wrist $\mathcal{F}_w$. To summarize the three cases,

$$\begin{aligned} \mathcal{F}_a &= 1, \\ \mathcal{F}_b &= \mathcal{F}_h \mathcal{F}_e, \text{and} \\ \mathcal{F}_c &= \mathcal{F}_h \mathcal{F}_w. \end{aligned}$$

We plan to obtain user performance data by repeating the peg-in-hole tasks using the telemanipulation scenario. If we assume that some real psychophysical measure of performance $\mathcal{P}$, $e.g.$, task completion time, peg-in-hole force variability, etc., is proportional to $\mathcal{F}$, then we have a way of assessing the fidelity $\mathcal{F}_e$ of the virtual environment. Since the haptic master and slave wrist have essentially the same characteristics, $\mathcal{F}_h \approx \mathcal{F}_w$, and therefore $\mathcal{F}_c \approx 2\mathcal{F}_h$. By examining the ratio of performances $\mathcal{P}_b$ and $\mathcal{P}_c$,

---

*JR3, Inc. `http:www.jr3.com`.

we obtain

$$\mathcal{F}_e \approx 2\mathcal{F}_b/\mathcal{F}_c \approx \mathcal{P}_b/\mathcal{P}_c.$$

Thus a meaningful numerical value, $0 \leq \mathcal{F}_e \leq 1$, can be assigned representing the degree of reality provided by the virtual environment. This will be possible because the influence of the haptic master itself has been effectively "removed" from the experimental setting.

5 Preliminary Results

We have to date obtained quantitative results for a peg-in-hole task in the real and virtual scenarios, and anecdotal results for the remote-real scenario. Preliminary findings indicate that task performance is best in a real environment. 90 trials were recorded for the real task scenario and 89 trials for the virtual task scenario. Operators performed the real peg-in-hole task faster and more accurately than the virtual one. Terminal forces (forces in the last 1s of a trial) applied by operators in both scenarios were not significantly different in any axis. However, the variability of force application during any given trial, as measured by "within trial" terminal force standard deviation (σ), was greater for the virtual haptic task [14]. The telemanipulation system has been used successfully in the remote-real scenario to perform a peg-in-hole task. The system is first used in an indexed coarse-fine mode to perform approximate alignment of the peg with the hole and then switched to proportional mode for final alignment. The user can convincingly feel contact of the peg with the surface and edges around the rim of the hole. There are some instabilities, however, and the PUMA is currently only operated in translation. These issues will be addressed before experimental trials are begun with subjects.

6 Conclusion

We have presented a high-fidelity system for evaluating haptic performance. We project that quantitative analysis of the strategies employed during operator performance of the same given task in all three scenarios discussed will yield significant insight into improved haptic interface design and rendering techniques.

Aknowledgements

References

[1] R. Ellis, O. Ismaeil, and M. Lipsett, "Design and evaluation of a high-performance haptic interface," *Robotica*, vol. 14, pp. 321–327, 1996.

[2] P.Richard, A. Kheddar, and R. England, "Human performance evaluation of two handle haptic devices in a dextrous virtual telemanipulation task," *Proceeding of the 1999 IEEE/RSJ International Conference on Intelligent Robots and Systems*, pp. 1543–1548, 1999.

[3] P. Buttolo, D. Kung, and B. Hannaford, "Manipulation in real, virtual and remote environments," *Proceedings IEEE Conference on System, Man and Cybernetics*, vol. 5, pp. 4656–61, October 1995.

[4] B. Hannaford, L. Wood, D. McAffee, and H. Zak, "Performance evaluation of a six-axis generalized force-reflecting teleoperator," *IEEE Transactions on Systems, Man, and Cybernetics*, vol. 21, May/June 1991.

[5] T. Yoshikawa and K. Yoshimoto, "Haptic simulation of assembly operation in virtual environment," in *Proc. ASME Dynamic Systems and Control Division*, vol. 69-2, pp. 1191–1198, ASME, 2000.

[6] B. J. Unger, A. Nicolaidis, P. J. Berkelman, A. Thompson, R. L. Klatzky, and R. L. Hollis, "Comparison of 3-D haptic peg-in-hole tasks in real and virtual environments," in *Proc. Int'l. Symp. on Intelligent Robots and Systems*, (Maui, Hawaii), Oct. 29—Nov. 3 2001.

[7] R. L. Hollis and S. E. Salcudean, "Lorentz levitation technology: a new approach to fine motion robotics, teleoperation, haptic interfaces, and vibration isolation," in *Proc. 6th Int'l Symposium on Robotics Research*, (Hidden Valley, PA), October 2-5 1993.

[8] S. E. Salcudean, N. M. Wong, and R. L. Hollis, "Design and control of a force-reflecting teleoperation system with magnetically levitated master and wrist," *IEEE Trans. on Robotics and Automation*, vol. 11, pp. 844–858, December 1995.

[9] R. L. Hollis, A. P. Allan, and S. Salcudean, "A six-degree-of-freedom magnetically levitated variable compliance fine motion wrist," in *4th Int'l Symposium on Robotics Research*, (Santa Cruz, CA), August 9-14 1987.

[10] R. L. Hollis, S. Salcudean, and A. P. Allan, "A six-degree-of-freedom magnetically levitated variable compliance fine motion wrist: Design, modeling, and control," *IEEE Transactions on Robotics and Automation*, vol. 7, pp. 320–332, June 1991.

[11] E. D. Fasse, "On the spatial impedance control of levitated platforms," in *4th IFAC Nonlinear Control Systems Design Symposium, NOLCOS '98*, vol. 3, pp. 601–6, Elsevier Science, 1998.

[12] P. J. Berkelman and R. L. Hollis, "Lorentz magnetic levitation for haptic interaction: Device design, performance, and interaction with physical simulations," *Int'l. J. of Robotics Research*, vol. 19, pp. 644–667, July 2000.

[13] D. Baraff, *Coriolis v1.227 Documentation*, September 1997.

[14] B. J. Unger, A. Nicolaidis, P. J. Berkelman, A. Thompson, S. Lederman, R. L. Klatzky, and R. L. Hollis, "Virtual peg-in-hole performance using a 6-DOF magnetic levitation haptic device: Comparison with real forces and visual guidance alone," in *10th Int'l. Symp. on Haptic Interfaces for Virtual Environments and Teleoperator Systems*, (Orlando, FL), pp. 263–270, March 2002.